

****Volume Title****
*ASP Conference Series, Vol. **Volume Number***
****Author****
 © ****Copyright Year**** *Astronomical Society of the Pacific*

Observations of Supersonic Downflows Near the Umbra-Penumbra Boundary of Sunspots as Revealed by Hinode

Rohan E. Louis¹, Luis R. Bellot Rubio², Shibu K. Mathew¹, P. Venkatakrisnan¹

¹*Udaipur Solar Observatory, Physical Research Laboratory Dewali, Badi Road, Udaipur, Rajasthan - 313004, India*

²*Instituto de Astrofísica de Andalucía (CSIC), Apartado de Correos 3004, 18080 Granada, Spain*

Abstract. High resolution spectropolarimetric observations by Hinode reveal the existence of supersonic downflows at the umbra-penumbra boundary of 3 sunspots that was recently reported by Louis et al. (2010). These downflows are observed to be co-spatial with bright penumbral filaments and occupy an area greater than 1.6 arcsec^2 . They are located at the center-side penumbra and have the same polarity as the sunspot which suggests that they are not associated with the Evershed Flow. In this paper we describe the supersonic velocities observed in NOAA AR 10923 and discuss the photospheric as well as chromospheric brightenings, that lie close to the downflowing areas. Our observations suggest that this phenomenon is driven by dynamic and energetic physical processes in the inner penumbra which affect the overlying chromosphere and thus provide new insights for numerical models of sunspots.

1. Introduction

The Evershed flow (EF; Evershed 1909) can be regarded as a signature property of sunspot penumbrae (Solanki 2003, and references therein) that exemplifies the latter's filamentary structure. In the inner penumbra the EF starts as upflows (Bellot Rubio et al. 2006; Rimmele & Marino 2006; Franz & Schlichenmaier 2009) that turns into downflows in the mid and outer penumbra (Westendorp Plaza et al. 1997; Schlichenmaier & Schmidt 1999; Mathew et al. 2003; Bellot Rubio et al. 2004).

In addition to the EF, other types of mass motions exist in the penumbra, as reported recently by Katsukawa & Jurčák (2010) using Hinode observations. They detect small-scale downflowing patches with velocities of $\approx 1 \text{ km s}^{-1}$ which have the same polarity as the parent sunspot. Some of them also appear to be co-spatial with chromospheric brightenings. Based on their physical properties Katsukawa & Jurčák (2010) infer that these weak downflows are different from the Evershed mass returning to the photosphere, which sometimes happens well within the penumbra (Bellot Rubio et al. 2004, 2007; Sainz Dalda & Bellot Rubio 2008).

Louis et al. (2010) observed a new type of downflows which are supersonic and occur at or near the umbra-penumbra boundary of sunspots. These downflowing patches are conspicuously large in size with areas ranging from $1.6\text{-}6 \text{ arcsec}^2$. They have the same polarity as the sunspot and occur along bright penumbral filaments. Their prop-

erties are different from those of the Evershed flow and the downflows reported by Katsukawa & Jurčák (2010), which indicates a different physical origin. The strong downflows possibly represent energetic and dynamic processes occurring in the inner penumbra which affect the chromosphere. In this paper we restrict our confine our discussion to the supersonic downflows observed in NOAA AR 10923 and briefly describe the photospheric as well as chromospheric activity associated with the supersonic downflows.

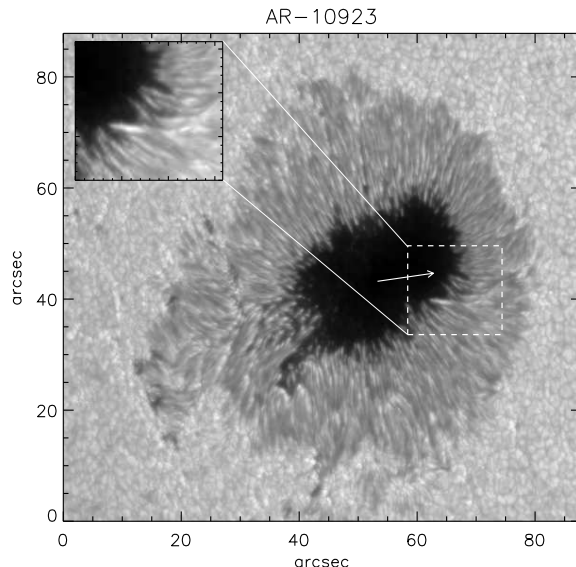


Figure 1. Continuum image of NOAA AR 10923 at 630 nm. The white dashed square represents the small region chosen for analysis and whose magnified image is shown in the inset. The white arrow points to disk center.

2. Observations

High resolution spectro-polarimetric observations of NOAA AR 10923 were carried out using the Solar Optical Telescope (SOT; Tsuneta et al. 2008) on board Hinode (Kosugi et al. 2007) on 2006 November 10 when the sunspot was located at a heliocentric angle of 50° as shown in Figure 1. The AR was mapped by the spectro-polarimeter (SP; Lites et al. 2001; Ichimoto et al. 2008) from 16:01 UT to 17:25 UT in the normal mapping mode with an exposure time of 4.8 s and a pixel size of $0''.16$. The four Stokes profiles of the neutral iron lines at 630 nm were recorded with a spectral sampling of $21.55 \text{ m}\text{\AA}$ at each slit position. In addition to the Stokes spectra, G-band and Ca II H filtergrams acquired by the Broadband Filter Imager (BFI) close to the SP scans were also employed. The filtergrams had a sampling of $0.''055$ with a cadence of 30 s. These data were recorded from 13:00 to 14:00 UT.

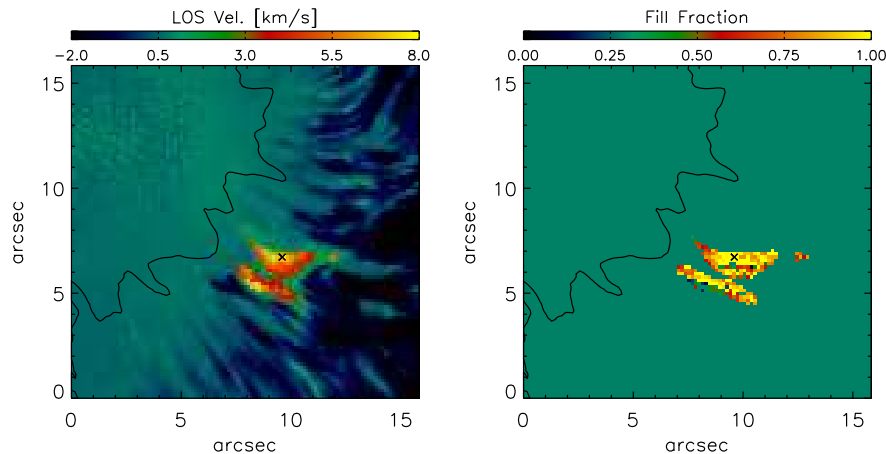


Figure 2. **Left:** LOS velocity derived from SIR combining 1 component and 2 component inversions. **Right:** The fill fraction of the fast component. The black contour depicts the umbra-penumbra boundary. Both images have been scaled as shown in their respective colour bars. The black cross corresponds to the pixel exhibiting supersonic velocity. The Stokes profiles emanating from this pixel are shown in Figure 3.

3. Results

3.1. Supersonic downflows from SIR inversions

The detection of the supersonic downflows was carried out by constructing red and blue wing magnetograms at ± 34.4 pm from the line center of 630.25 nm Fe line as described in Louis et al. (2010). The far wing magnetograms are useful to detect pixels with strong downflows but do not yield the magnitude of the velocities present in those locations. In order to ascertain the velocities, the observed Stokes profiles were subject to an inversion using the SIR code (Stokes Inversion based on Response Functions; Ruiz Cobo & del Toro Iniesta 1992). Two sets of inversions were carried out to determine the velocities. In the first run, a single magnetic component was assumed in each pixel with the vector magnetic field (field strength, inclination and azimuth) and LOS velocity remaining constant with height. The resultant LOS velocity map is shown in Figure 2 of Louis et al. (2010). Pixels exhibiting velocities greater than 2 km s^{-1} were then selected and subjected to a second set of inversions in which two magnetic components were assumed to co-exist in a single resolution element, both of which had height independent physical parameters. The one and two component SIR inversions also retrieved height-independent micro- and macro-turbulent velocities as well as the fraction of stray light in each pixel. The left panel of Figure 2 shows the LOS velocity combining both the inversion sets, while the fill fraction of the fast component is depicted on the right.

Figure 2 depicts supersonic downflows $\sim 8 \text{ km s}^{-1}$ in AR 10923 located nearly $3''$ from the umbra-penumbra boundary. To the best of our knowledge these are the largest downflows ever detected in the inner penumbra lying close to the umbra-penumbra interface. The right panel of the figure indicates that a large fraction of the resolution element is dominated by the stronger downflowing component. We estimate the typical

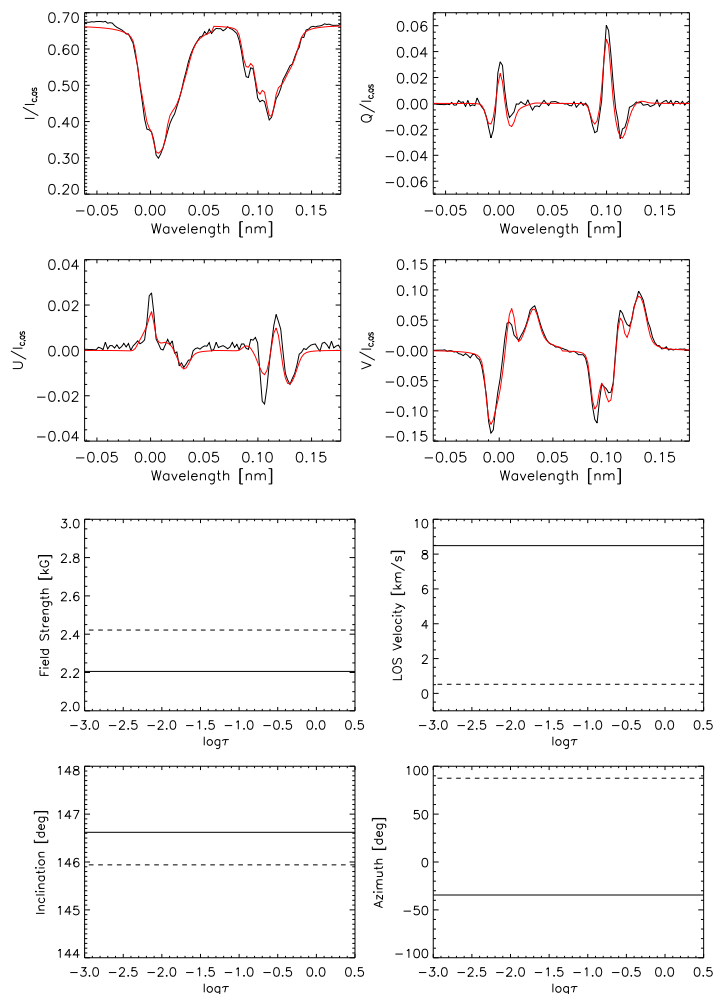


Figure 3. **First and second rows:** Observed (*solid*) and best-fit (*red*) Stokes profiles of the pixel marked in Figure 2 using a two-component model. **Third and fourth rows:** The height independent stratification of the physical parameters corresponding to the two-components shown as *solid* and *dashed* lines.

size of the downflowing patch to be $\approx 1.6 \text{ arcsec}^2$. The strong downflowing zones are surrounded by upflows measuring 2 km s^{-1} which can be identified with the Evershed flow.

The Stokes V profile emerging from the downflowing regions exhibit a satellite red lobe while the Stokes I profile have highly inclined red wings, as illustrated in Figure 3 for the pixel marked with the cross in Figure 2. The above spectral characteristics are reproduced satisfactorily by the two-component inversions. These two magnetic components could either reside side-by-side in the same resolution element or could be stacked one on top of the other. While the exact configuration remains uncertain, supersonic velocities exist in the presence of very strong magnetic fields as indicated in the third row of Figure 3. In addition, the polarity of the strong downflowing component is the same as that of the parent sunspot, which rules out the possibility of them being Evershed flows returning to the solar surface. The strong fields exceeding 2 kG would

also inhibit convection and this would suggest that the downflows are likely to be caused by an alternative mechanism.

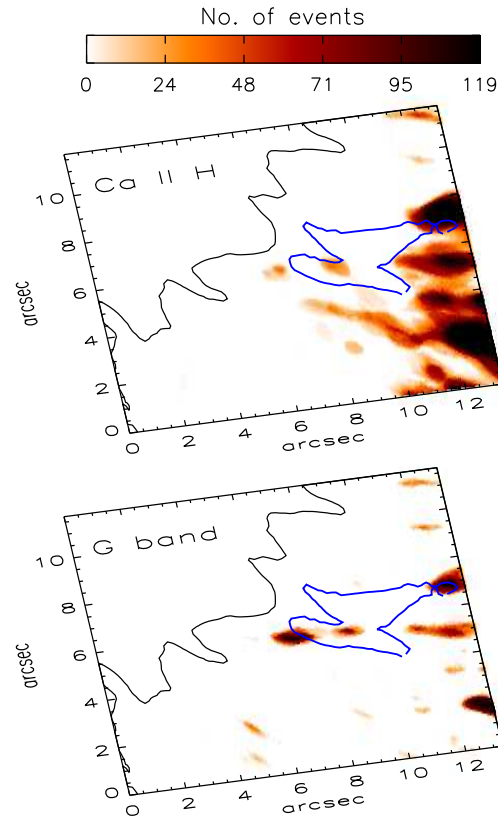


Figure 4. G-band (*bottom*) and Ca (*top*) event maps depicting locations with intensity close to the quiet Sun photosphere. Blue contours of LOS velocity greater than 2 km s^{-1} have been overlaid on the filtergrams. The black contour corresponds to the continuum intensity at 630 nm. The images have been scaled as shown by the horizontal color bar.

3.2. Photospheric and Chromospheric Brightenings

We now turn our attention to the photospheric and chromospheric brightenings associated with the supersonic downflows. These brightness enhancements are observed to lie in close proximity to the downflowing patches and can have intensities comparable to the quiet Sun. The penumbral filament near one of the downflowing zones has an intensity of $0.9I_{\text{QS}}$ as seen from the continuum image at 630 nm (see inset of Figure 1). Higher up in the chromosphere, these brightenings are $\sim 77\%$ more intense than the penumbral microjets (MJs), which appear to be in the decay phase (Ryutova et al. 2008b). While the brightness enhancements, seen near the supersonic downflows, appear as isolated blobs on the filaments, MJs are oriented nearly perpendicular to the filament (see Figure 4 of Ryutova et al. (2008b)).

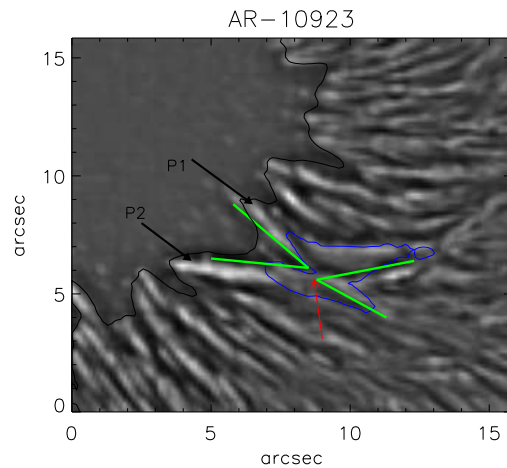


Figure 5. Continuum image that has been unsharp masked using a 3×3 pixel box-car. The red arrow indicates the location where the filaments P1 and P2 appear to intersect each other. The solid green lines refer to the bisecting angles between the filaments P1 and P2. The blue contour has been drawn for LOS velocities greater than 2 km s^{-1} .

To determine if the proximity of the enhancements to the downflows endures with time, event maps were constructed in the photosphere as well as chromosphere using the G band and Ca filtergram time sequence. The procedure has been described in Louis et al. (2010) with threshold values of 0.85 and 0.9 being employed for the photosphere and chromosphere respectively. The resulting event maps are shown in Figure 4 which have been stacked one on top of the other.

At both heights we find a large number of events concentrated near the downflows resembling blobs that were seen in the individual filtergrams. While the brightenings in the photosphere persist for the entire 1 hr sequence, this is limited to nearly one-third of the time duration in the chromosphere. More importantly, the enhancements appear very similar in shape and are nearly co-spatial. The use of a large threshold in the chromospheric event map, removes all signatures of the relatively weaker and transient MJJs.

4. Discussion

The downflows that are associated with the EF can sometimes be supersonic in the outer penumbra (del Toro Iniesta et al. 2001; Bellot Rubio et al. 2004) or even beyond the sunspot boundary (Martínez Pillet et al. 2009). Such a configuration represents mass flux returning to the photosphere and has a polarity opposite to that of the sunspot. The supersonic downflows we have observed have the same polarity as the parent sunspot and so they cannot be related to the Evershed downflows. One could assume that these strong downflows are the photospheric counterpart of some kind of inverse Evershed flow seen in the chromosphere. However, it is speculative as to how such a chromospheric phenomenon could produce supersonic downflows in the inner penumbra at the photosphere.

The orientation of the filaments P1 and P2, bifurcating at the strong downflowing patch (Figure 5), resemble the post reconnection configuration illustrated in Figure 5c of Ryutova et al. (2008a), suggesting that the origin of the downflows is the slingshot effect associated with the reconnection of the filaments. The bisecting angles shown by the solid green lines were estimated to be $\approx 51^\circ$ and 46° respectively.

According to Ryutova et al. (2008a), the unwinding of filaments in a cork screw fashion can lead to reconnection, transient brightenings and twists in the penumbral filaments. This model was proposed as a possible mechanism for producing the MJs. Magara (2010) investigated the above scenario using numerical simulations and concluded that MJs occur in the intermediate region between nearly horizontal flux tubes and the relatively vertical background field of the penumbra. In the model, only parts and not the entire penumbral filament participate in the reconnection process.

Slingshot reconnection may be a possible mechanism for producing the supersonic downflows and the photospheric as well as chromospheric brightenings, although there is no strict one-to-one correspondence between the two phenomenon. The above process has to be different from the one producing MJs since their intensities and lifetimes are much smaller than the events described in this work.

5. Summary

High resolution spectro-polarimetric observations of NOAA AR 10923 taken with Hinode reveals supersonic downflows near the umbra-penumbra boundary. The downflows are observed in large patches having an area of 1.5 arcsec^2 . Using a 2 component model atmosphere the SIR code retrieves supersonic values 8 km s^{-1} . These downflows are the largest velocities ever detected at these locations in a sunspot. Frequent occurrences of strong downflows at the border of an umbra without a penumbra has been reported by Shimizu et al. (2008).

The strong velocities are observed to have 2 kG magnetic fields which have the same polarity as the sunspot. This would imply that the downflows are not related to the Evershed flow, although the latter could be separately present at those locations. We find intense and long lived chromospheric brightenings near the strong photospheric downflows extending over an area of $\approx 1\text{--}2 \text{ arcsec}^2$. Furthermore, photospheric brightenings nearly as intense as the quiet Sun are also present in the downflowing regions or close to them. These downflows may have lifetimes of up to 14 hr (or more) as validated from several consecutive Hinode/SP scans (Louis et al. 2010).

The penumbral filaments in the vicinity of the strong downflows appear to be twisted in the manner described by Ryutova et al. (2008b) that would arise from a reconnection process. Such a process could produce the transient penumbral microjets. These events are ubiquitous in the penumbra and the photospheric downflows observed with them are typically 1 km s^{-1} , as reported by Katsukawa & Jurčák (2010). The chromospheric brightenings described in Section 3.2 however, are more stronger, bigger and long lived than the microjets. The supersonic downflows that we have observed are an entirely new phenomenon. They are possibly driven by dynamic and very energetic processes occurring in the inner penumbra which produce highly intense and long lived brightenings in the photosphere as well as in the chromosphere. A suitable theory is yet to be formulated for explaining these events and will be a challenge for future numerical models of sunspots.

Acknowledgments. We sincerely thank the Hinode team for providing the high resolution data. Hinode is a Japanese mission developed and launched by ISAS/JAXA, with NAOJ as domestic partner and NASA and STFC (UK) as international partners. It is operated by these agencies in co-operation with ESA and NSC (Norway). We thank the organizers for a wonderful meeting and for their warm hospitality.

References

- Bellot Rubio, L. R., Balthasar, H., & Collados, M. 2004, *A&A*, 427, 319
- Bellot Rubio, L. R., Schlichenmaier, R., & Tritschler, A. 2006, *A&A*, 453, 1117. arXiv:astro-ph/0601423
- Bellot Rubio, L. R., Tsuneta, S., Ichimoto, K., Katsukawa, Y., Lites, B. W., Nagata, S., Shimizu, T., Shine, R. A., Suematsu, Y., Tarbell, T. D., Title, A. M., & del Toro Iniesta, J. C. 2007, *ApJ*, 668, L91. 0708.2791
- del Toro Iniesta, J. C., Bellot Rubio, L. R., & Collados, M. 2001, *ApJ*, 549, L139
- Evershed, J. 1909, *MNRAS*, 69, 454
- Franz, M., & Schlichenmaier, R. 2009, *A&A*, 508, 1453. 0909.4744
- Ichimoto, K., Lites, B., Elmore, D., Suematsu, Y., Tsuneta, S., Katsukawa, Y., Shimizu, T., Shine, R., Tarbell, T., Title, A., Kiyohara, J., Shinoda, K., Card, G., Lecinski, A., Streander, K., Nakagiri, M., Miyashita, M., Noguchi, M., Hoffmann, C., & Cruz, T. 2008, *Solar Phys.*, 249, 233
- Katsukawa, Y., & Jurčák, J. 2010, *A&A*, 524, A20+. 1007.1702
- Kosugi, T., Matsuzaki, K., Sakao, T., Shimizu, T., Sone, Y., Tachikawa, S., Hashimoto, T., Minesugi, K., Ohnishi, A., Yamada, T., Tsuneta, S., Hara, H., Ichimoto, K., Suematsu, Y., Shimojo, M., Watanabe, T., Shimada, S., Davis, J. M., Hill, L. D., Owens, J. K., Title, A. M., Culhane, J. L., Harra, L. K., Doschek, G. A., & Golub, L. 2007, *Solar Phys.*, 243, 3
- Lites, B. W., Elmore, D. F., & Streander, K. V. 2001, in *Advanced Solar Polarimetry – Theory, Observation, and Instrumentation*, edited by M. Sigwarth, vol. 236 of *Astronomical Society of the Pacific Conference Series*, 33
- Louis, R. E., Bellot Rubio, L. R., Mathew, S. K., & Venkatakrishnan, P. 2010, *ArXiv e-prints*. 1010.0519
- Magara, T. 2010, *ApJ*, 715, L40
- Martínez Pillet, V., Katsukawa, Y., Puschmann, K. G., & Ruiz Cobo, B. 2009, *ApJ*, 701, L79
- Mathew, S. K., Lagg, A., Solanki, S. K., Collados, M., Borrero, J. M., Berdyugina, S., Krupp, N., Woch, J., & Frutiger, C. 2003, *A&A*, 410, 695
- Rimmele, T., & Marino, J. 2006, *ApJ*, 646, 593
- Ruiz Cobo, B., & del Toro Iniesta, J. C. 1992, *ApJ*, 398, 375
- Ryutova, M., Berger, T., Frank, Z., & Title, A. 2008a, *ApJ*, 686, 1404
- Ryutova, M., Berger, T., & Title, A. 2008b, *ApJ*, 676, 1356
- Sainz Dalda, A., & Bellot Rubio, L. R. 2008, *A&A*, 481, L21. 0712.2983
- Schlichenmaier, R., & Schmidt, W. 1999, *A&A*, 349, L37
- Shimizu, T., Lites, B. W., Katsukawa, Y., Ichimoto, K., Suematsu, Y., Tsuneta, S., Nagata, S., Kubo, M., Shine, R. A., & Tarbell, T. D. 2008, *ApJ*, 680, 1467. 0804.1167
- Solanki, S. K. 2003, *A&A Rev.*, 11, 153
- Tsuneta, S., Ichimoto, K., Katsukawa, Y., Nagata, S., Otsubo, M., Shimizu, T., Suematsu, Y., Nakagiri, M., Noguchi, M., Tarbell, T., Title, A., Shine, R., Rosenberg, W., Hoffmann, C., Jurcevich, B., Kushner, G., Levay, M., Lites, B., Elmore, D., Matsushita, T., Kawaguchi, N., Saito, H., Mikami, I., Hill, L. D., & Owens, J. K. 2008, *Solar Phys.*, 249, 167. 0711.1715
- Westendorp Plaza, C., del Toro Iniesta, J. C., Ruiz Cobo, B., Martínez Pillet, V., Lites, B. W., & Skumanich, A. 1997, *Nat*, 389, 47